Terr. Atmos. Ocean. Sci., Vol. 28, No. 3, 463-478, June 2017 doi: 10.3319/TAO.2016.10.26.01

Climate change impact assessment on Zhoshui River water supply in Taiwan

Jyun-Long Lee and Wen-Cheng Huang *

Department of Harbor and River Engineering, National Taiwan Ocean University, Keelung City, Taiwan

Article history:
Received 17 May 2016
Revised 23 September 2016
Accepted 26 October 2016

Keywords:
Climate change, Irrigation water requirement, Water shortages, Impact assessment

Citation:
Lee, J.-L. and W.-C. Huang, 2017: Climate change impact assessment on Zhoshui River water supply in Taiwan. Terr. Atmos. Ocean. Sci., 28, 463-478, doi: 10.3319/TAO.2016.10.26.01

ABSTRACT

This study evaluates the impact of climate change on water resources. An integrated procedure is proposed for assessing the water resources system response to climate change on the basin scale. The Zhoshui River basin in Central Taiwan was selected for the impact assessment. Five downscaled general circulation models based on the A1B scenario for 2046 - 2065 were adopted to assess the climate change impact, including (1) the irrigation water requirement downstream of the basin, (2) the river flow upstream of the basin, and (3) the water resources utilization related to supply and demand in the basin. Rising temperatures will cause the irrigation water requirement to increase by 10%. Precipitation in the basin will substantially decrease and likely cause a 20% decrease in river flow. Thus, irrigation water shortages may become more severe in the future. As an adaptation, the Hushan Reservoir, which will begin operation in mid-2016, can assist in offsetting domestic and industrial demand. To maintain the irrigation deficit at the present level (2001 - 2010) in the future, conveyance losses should reduce to 30% and the farming area used in the second paddy growth season should be decreased by 10%.

1. INTRODUCTION

The Intergovernmental Panel on Climate Change (IPCC) has stated that the observed increase in global average temperature since the mid-20th century is very likely due to the observed increases in anthropogenic greenhouse gas concentrations (IPCC 2007). Climate change has led to increased temperature, rising sea levels, and increased rainfall intensity. Thus, we will face more extreme weather events in the future.

Taiwan, located in the West Pacific, is a climate change impact hot spot. Some studies indicated that Taiwan's surface temperature will rise in the future (Lin et al. 2009; Hsu et al. 2011). The temporal precipitation distribution may become more uneven, and rainless days might occur more frequently (Huang et al. 2012, 2014a). The changes in hydrologic projections indicate that water resources management in Taiwan could become a challenging task. The climate change impact on the Shihmen Reservoir water supply in Northern Taiwan has been assessed by numerous authors (Lee and Huang 2014; Huang et al. 2014b). The results show that reduced inflow and increased demand will result in drought for the Shihmen Reservoir supply zone.

The purpose of this study is to assess climate change effects on water resources in the Zhoshui River basin in the Changhua and Yunlin areas of Central Taiwan (Fig. 1). This area is crucial for rice production in Taiwan. However, the area has suffered from severe land subsidence (Tung and Hu 2012; Hung et al. 2012), limiting the potential for groundwater pumping. Therefore, understanding the impact of climate change on this area's water resources system is essential.

The Zhoshui River originates in the Central Mountain Range. Figure 1 shows the Zhoshui River basin water resources infrastructure. Figure 2 depicts the basin water resources system. The Wushe Reservoir has a catchment area of 219 km^2 and is used for hydropower. Its operating rule curve (Fig. 3a) indicates that the reservoir will generate as much electricity as possible if the water surface level is above the rule curve. Otherwise, it will generate electricity according to the inflow. The Wujie Dam raises the water level and conveys water to the Sun-Moon-Lake Reservoir. Sun-Moon-Lake is the largest off-site reservoir in this basin. Although pumped-storage hydroelectricity is its main objective, it supports the water supply when the water from the main stream cannot satisfy the demand. Figure 3b indicates that if the Sun-Moon-Lake Reservoir water surface

* *Corresponding author*
E-mail: b0137@mail.ntou.edu.tw

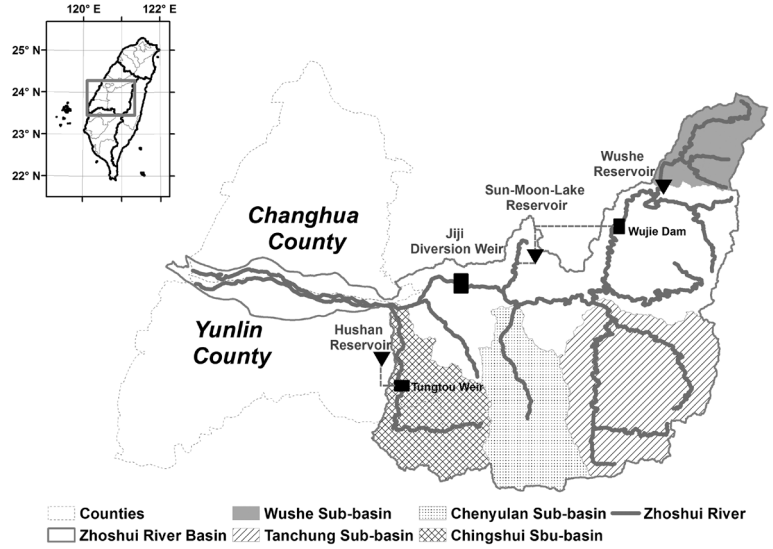

Fig. 1. Location and related water resource infrastructures of the study area.

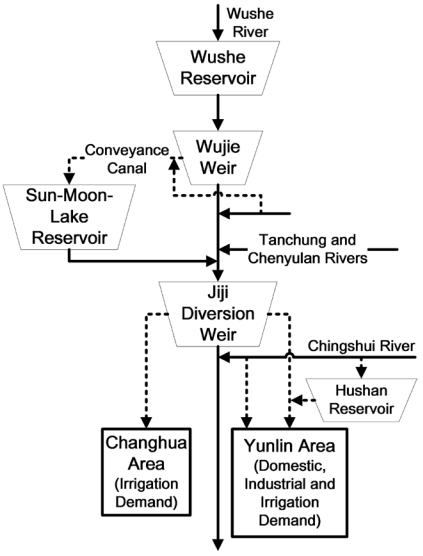

Fig. 2. Conceptual water resources system of the Zhoshui River Basin.

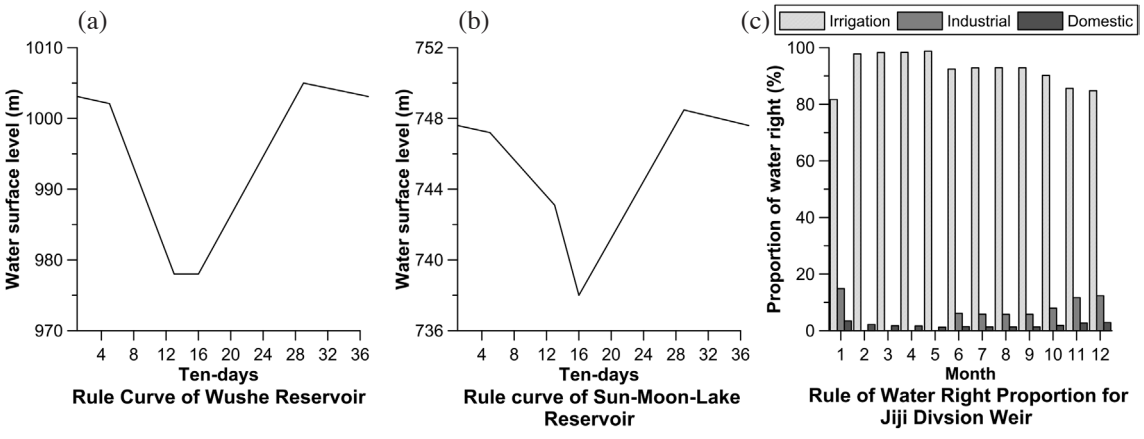

Fig. 3. The operation rules for (a) Wushe reservoir, (b) Sun-moon-lake reservoir, and (c) Jiji division weir.

level is over the rule curve, the reservoir release meets the maximum hydropower and downstream use requirements. Otherwise, it is at the minimum level for hydropower and downstream requirements. There are two tributaries in the midstream section, the Tanchung and Chenyulan Rivers, which encompass 700 and 450 km^2, respectively. The water resources in the upstream and midstream section eventually converge into the Jiji Division weir (with a catchment area of 2304 km^2). This weir is the Zhoshui River basin management center and is responsible for the Changhua and Yunlin area demand. If the Jiji Division weir storage is lower than the total demand, the release for different water users (irrigation, domestic, and industrial) should be in accordance with their water rights (Fig. 3c). Industrial users have no water rights from February through May.

Hushan is a newly built reservoir with a catchment area of 259 km^2. It is an off-site reservoir and receives Chingshui River flow from the intake at the Tungtou weir. The main task of this reservoir is to satisfy domestic demand and reduce groundwater pumping in Yunlin.

In the impact assessment performed in this study, we (1) calculated the Changhua and Yulin irrigation water requirements (in which agriculture is the main sector), (2) estimated the Zhoshui River basin streamflow, and (3) simulated the water resources system according to hydrological data. We then assessed the impact of climate change through a comparison between the present (2001 - 2010) and the future (2046 - 2065).

2. DATA AND METHODS

2.1 Meteorological Projections

General circulation models (GCMs) are the most advanced tools available for simulating the global climate system response to increasing greenhouse gas concentrations. This study focuses on the projected conditions for the years 2046 - 2065. Meteorological data projections (precipitation and temperature) based on the A1B scenario (Nakicenovic and Swart 2000) were adopted from the following five GCMs: (1) CGCm3 from the Canadian Center for Climate Modeling and Analysis (CCCma), (2) Cm3 from the Centre National de Recherches Meteorologiques (CNRM), (3) Mk3.0 from Australia's Commonwealth Scientific and Industrial Research Organization (CSIRO), (4) Cm2.0 from the Geophysical Fluid Dynamics Laboratory (GFDL), and (5) FGOALS-g1.0 from the State Key Laboratory of Numerical Modeling for Atmospheric Sciences and Geophysical Fluid Dynamics (LASG). The original GCM outputs have coarse resolutions that cannot be directly applied to watershed scale calculations. Statistical downscaling from GCM scenario-run grids to local meteorological stations is therefore necessary. We obtained the aforementioned GCM downscaled projections from the Global Change Research Center of National Taiwan University. The downscaling process can be briefly explained as follows: (1) the GCM output near Taiwan was adjusted with respect to the National Centers for Environmental Prediction (NCEP) reanalysis data through the training period by linking the normalized probability distribution function of the mean climate parameters; (2) transfer functions such as multiple-variant linear regression were established to link the NCEP reanalysis variants with local records through the training period; (3) meteorological projections at each station through the verification period were adjusted with respect to local records using the first stage procedure, and the established linkage was then extended to adjust the forward projection. For more downscaling process details, please refer to Kalnay et al. (1996) and Lin et al. (2009, 2010).

2.2 Paddy Water Requirement

The crop water requirement relates directly to the crop variety and the field evapotranspiration. The Food and Agriculture Organization (FAO) of the United Nations uses the following equation to estimate the crop water requirement grown in large fields under disease-free and well-fertilized conditions (Allen et al. 2006):

$$ET_c = K_c \times ET_o \tag{1}$$

where ET_c and ET_o are the crop and reference evapotranspiration (mm day^{-1}), respectively, and K_c is a crop coefficient (dimensionless).

K_c is based on a distribution instead of a constant throughout the growth duration and differs depending on the crop variety. Shih et al. (1996) proposed a K_c for paddy rice in Taiwan; the K_c values for the first and second cropping seasons are shown in Table 1.

To estimate reference evapotranspiration, ET_o, the FAO Penman-Monteith (PM) equation is recommended (Allen et al. 2006):

$$ET_o = \frac{0.408\Delta(R_n - G) + \gamma \frac{900}{T + 273} u_2 (e_s - e_a)}{\Delta + \gamma(1 + 0.34u_2)} \tag{2}$$

where Δ and γ are the saturation vapor pressure curve slope and the psychrometric constant (kPa °C^{-1}), respectively. R_n and G are the net radiation at the crop surface and the soil heat flux density (MJ m^{2}day^{-1}), respectively. T is the mean daily air temperature at a height of 2 m (°C). e_s and e_a are the saturation and actual vapor pressure (kPa), respectively. u_2 is the wind speed at a height of 2 m (m s^{-1}).

Because only daily temperature and precipitation are available from the GCM projections, information for the PM equation is insufficient for evapotranspiration estimation for future scenarios. Instead, the Hamon method, a

temperature-based equation for estimating evapotranspiration, was used (Shaw and Riha 2011):

$$PE = 29.8N_h \frac{e_s}{T + 273.2} \quad (3)$$

where PE is the potential evapotranspiration according to the Hamon method (mm day^{-1}) and N_h is the sunshine duration (hours). The theoretical future N_h was defined as in Allen et al. (2006).

2.3 Bias Correction

ET_o is regarded as a standard to be followed; therefore, the estimated PE value must be corrected. The quadrant transformation method (Huang et al. 2012) was applied in this study for bias correction. Figure 4 shows the quadrant transformation method concept, in which the curve indicates the percentage of time that evapotranspiration is equaled or exceeded during the period of study. The difference between the first and fourth quadrants was estimated from observations or projections, whereas the difference between the third and fourth quadrants was due to climate change. The curve in the second quadrant yields the corrected PE and was produced by conversions in the other three quadrants.

The bias correction process can be described by the following steps: (1) constructing the curves that indicate the percentage of time equaled or exceeded (Searcy 1959) in the first (observations in the present), third (projections in the future), and fourth (projections in the present) quadrants; (2) determining the corresponding percentile in the fourth quadrant using the given projection in the third quadrant; (3) finding a new value in the first quadrant and point in the second quadrant based on the percentile; and (4) repeating steps (2) and (3) to obtain the curve for the correction in the second quadrant.

Monthly bias correction was adopted in this study

Table 1. K_c distribution, accumulation of growing degree days and limit of ponding storage for growth stages of paddy rice.

Growth stages	K_c in the first cropping season (February - June)	K_c in the second cropping season (July - November)	Accumulation of growing degree days (°C-days)	Lower limit of tolerable ponding depth (mm)	Upper limit of tolerable ponding depth (mm)
Vegetative stage I	0.5	0.9	269	30	50
Vegetative stage II	0.8	1.2	538	20	30
Vegetative stage III	1.2	1.5	807	0	20
Reproductive stage I	1.3	1.6	980	50	100
Reproductive stage II	1.3	1.5	1153	50	100
Ripening stage I	1.2	1.3	1343	50	100
Ripening stage II	1.1	1.1	1534	20	30
Ripening stage III	0.7	0.6	1725	0	20

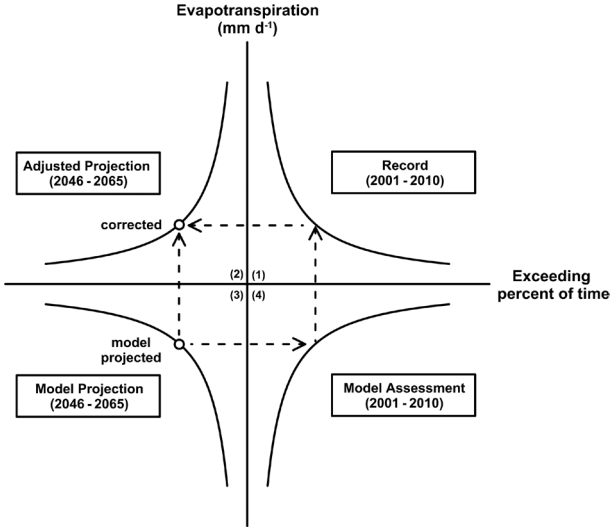

Fig. 4. Quadrant transformation method concept.

based on seasonal variations. The above statement could be expressed as the equation:

$$x^{F}_{crt.} = f^{P}_{obs.}{}^{-1}\left[f^{P}_{proj.}\left(x^{F}_{proj.}\right)\right] \tag{4}$$

where x is the daily potential evapotranspiration (mm); f and f^{-1} are the function and inverse function of the monthly curves that indicate the percentage of time equaled or exceeded. The superscripts P and F represent the present and future time, respectively; and the subscripts *obs*., *proj*., and *crt*. symbolize the observation data, GCMs projections, and corrected data, respectively.

2.4 Paddy Development Mechanism

Calendars are often used to predict crop development for management. However, calendar days can be misleading, particularly during early crop growth stages (Miller et al. 2001). In addition, climate change complicates using constant days to represent each growth stage.

Numerous studies have found that crop growth is directly related to temperature (Russelle et al. 1984; Eskridge and Stevens 1987). Therefore, the phenology crop model can be constructed according to the growing degree days (GDD) equation:

$$\begin{aligned} &\mathrm{GDD} = \sum(T - T_b)_i = \sum(\Delta T)_i \\ &\Delta T = 0 \ \text{ if } \ T - T_b \le 0 \end{aligned} \tag{5}$$

where T_b is the base temperature for a crop variety. ΔT is set to 0 if the daily temperature is less than T_b; thus, the crop stops developing at that time (Gilmore and Rogers 1958).

The GDD equation is a simple thermal time equation. It accumulates thermal time linearly with increasing temperature above a constant crop-specific base temperature. Theoretically, if thermal time is accumulated correctly for a given crop variety, crop development should then be directly related to thermal time accumulation (i.e., GDD). The GDD equation indicates that each crop growth stage is related to the accumulation of thermal time, regardless of the planting time or location (Hodges 1991).

For paddy rice, T_b is generally set to 10°C (Hardke et al. 2013). Moreover, the GDD accumulation value is set to 1725 °C-days according to recommendations for the common paddy variety in Taiwan (Hualien District Agricultural Research and Extension Station 2006, 2007). The GDD accumulation details for each paddy growth stage are shown in Table 1.

2.5 Irrigation Water Requirement

A paddy field water balance model is presented in Fig. 5. We applied it to calculate the irrigation water requirement. Considering different soil types in paddy fields and the irrigation canal water conveyance loss, the continuity equation for a paddy field is expressed as follows:

$$S_{t+1} = S_t + P_t - ET_{ct} - \sum_j f_j A_j{}^{\circ} + \frac{IR_t}{\sum_i A_i^{*}(1 + CL_i)} \tag{6}$$

where S_t, P_t, ET_{ct}, and IR_t indicate the daily water storage, rainfall, crop evapotranspiration, and irrigation water requirement in the paddy fields at time t (mm day^{-1}), respectively. f_j is the percolation rate of the jth soil type (mm day^{-1}), $A_j{}^{\circ}$ is the percentage of the jth soil type area (%), A_i^{*} denotes the percentage of total farming area controlled by the ith canal (%), and CL_i is the average water conveyance loss in the area controlled by the ith canal (%).

The irrigation water requirement must be externally supplied to offset the deficit for paddy growth when precipitation and storage do not satisfy water demand. By

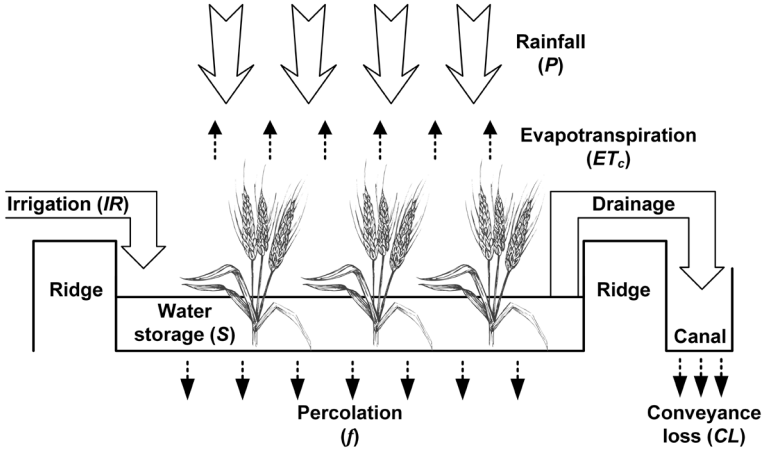

Fig. 5. Conceptual model for water balance in paddy fields.

contrast, the irrigation water requirement is 0 when demand is satisfied. Therefore, Eq. (6) can be rewritten as follows:

$$IR_t = \sum_i A_i^* (1 + CL^i) \cdot (ET_{ct} + \sum_j f^j A_j^\circ + S_t^{\min} - S_t - P_t)$$
$$\text{if } S_t + P_t - ET_{ct} - \sum_j f^j A_j^\circ < S_t^{\min} \quad (7)$$

The rainfall stored in the paddy field for growth is termed the effective rainfall (P_t^*) at time t; hence,

$$P_t^* = \min\left\{S_t^{\max} - S_t + ET_{ct} + \sum_j f_j A_j^\circ, P_t\right\} \quad (8)$$

where $S_t^{\max}$ and $S_t^{\min}$ are the upper and lower limits of tolerable ponding depth for paddy during different growth stages (mm), respectively (Table 1).

2.6 Rainfall-Runoff Model

The tank model (Sugawara 1961) was adopted to assess stream flow in the climate change context in this study. As the tank model is a conceptual and deterministic rainfall-runoff model composed of several tanks that accounts for a watershed storage effect. In other words, the tank model effective simulation performance is due to continuous damping and lagging effects (Lee 1993). The tank model advantages include a simple structure, easy calculations and reasonable functions (Yokoo and Kazama 2012).

Figure 6 shows the runoff mechanism for a 2-layer tank model. When precipitation reaches the height of ha_1 in the top tank, the watershed is saturated. If the water surface depth in the top tank is over ha_1, additional precipitation discharges from the tank through orifice a_1. This process is the major component of surface runoff. In a high-intensity storm, the top tank water surface depth is higher than ha_2. The outflow through orifice a_2 represents the runoff in this scenario. Orifice a_0 simulates the percolation process in a watershed, in which the water is transported into the ground. The bottom of the 2-layer tank model represents the interflow and groundwater and is opposite the top tank. Parameter hb_1 is a threshold that is similar to ha_1. The discharge through orifice b_1 represents the outflow of interflow and groundwater.

Six parameters in the 2-layer tank model require calibration. We used the multi-start Powell method to calibrate the tank model parameters. The Powell method is an efficient and robust conjugate direction method used to find the minimum of a function (Powell 1964). An inappropriate initial point converges toward a local minimum instead of a global minimum when the problem structure is more complex. As an improvement, the multi-start Powell method can overcome the Powell method disadvantages through providing several initial points. Tanakamaru (1995) suggested that the multi-start Powell method is an effective and powerful tool for tank model parameter calibration. Chen et al. (2005) recommended that the number of initial points should be equal to or more than 50 to avoid searching failure.

The parameter search boundaries for tank model calibration are shown in Table 2. If the orifice coefficient summation of each tank is more than 1, the tank outflow might be greater than the inflow and storage summation. To avoid this illogical relationship, the orifice coefficient of the top tank must be subject to the following equation during calibration:

$$a_0 + a_1 + a_2 \le 1 \quad (9)$$

Additionally, we selected the average percentage error as the objective function during tank model parameter calibration:

$$obj = \sum \frac{|Q_t^{obs} - Q_t^{sim}|}{Q_t^{obs}} \div N_d \quad (10)$$

where Q_t^{obs} and Q_t^{sim} are the observed and tank model-simulated discharges, respectively. N_d denotes the number of simulation days.

2.7 Simulation Assessment Indices

We used the degree of satisfaction, reliability and shortage index (SI) to represent the water resources simulation performance. The definition of these indices is provided in the following equations:

$$\text{degree of satisfaction} = \frac{SPL}{DM} \quad (11)$$

$$\text{degree of reliability} = \frac{N_s}{N_d} \quad (12)$$

$$SI = \frac{100}{N_y} \sum \left(1 - \frac{SPL}{DM}\right)^2 \quad (13)$$

where SPL and DM are the supplied water and water demand, respectively (m^3). N_s is the total satisfied days, and N_y indicates the simulation time in years.

3. MODEL VALIDATION

3.1 Validation of Bias Correction

Figure 7 shows the difference before and after bias correction for evapotranspiration. The curve distributions indicating the percentage of time equaled or exceeded between observations and projections in the present (first and fourth

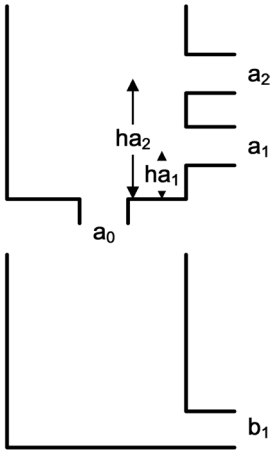

Fig. 6. A two-layer tank model.

Table 2. Searching boundaries of the two-layer tank model parameters.

Parameters	Orifice coefficient (day^{-1})				Orifice height (mm)	
	a_0	a_1	a_2	b_1	ha_1	ha_2
lower-upper boundary	0 - 1	0 - 1	0 - 1	0 - 1	0 - 500	0 - 500

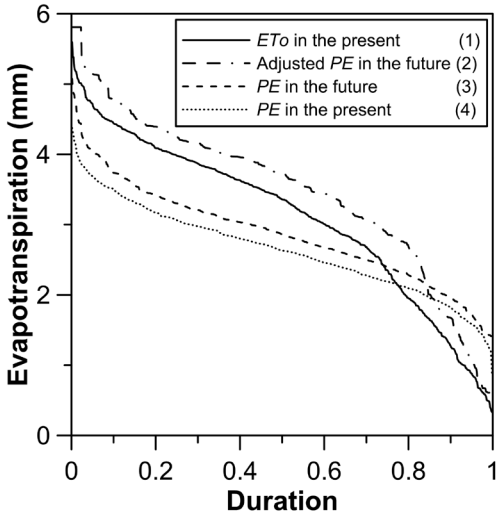

Fig. 7. Comparison of the exceeding percent time curves for evapotraspiration at each quadrant in March (LASG GCM).

quadrant) are quite different. However, after the quadrant transformation, the distribution of adjusted data (second quadrant) is more similar to the observations (first quadrant).

3.2 Water Balance Model Validation for Irrigation

Figure 8 shows the observed water consumption and estimated water requirements for paddy rice in the Changhua and Yunlin areas. The bias range is approximately 2.3 - 34.6% in Changhua and 0.2 - 87.8% in Yunlin. On average, the biases through the first and second paddy growth seasons (approximately February - June and July - November) are 10.8 and 16.1% in Changhua and 17.0 and 30.0% in Yunlin, respectively.

This difference might arise owing to variations in hydrological conditions. The irrigation consumption records are based on actual water received from canals, whereas the model estimations assume that irrigation requirements can be fulfilled with abundant water. For example, (1) there is considerable underestimation in 2002 in Yunlin in the second paddy growth season (Fig. 8d). Because 2002 was a dry year, managers decided to transfer most of the water to Changhua rather than Yunlin (Fig. 8b); (2) there is overestimation in Yunlin throughout 2005 and 2006 because these two years were wet, and more water could be supplied to Yunlin (Figs. 8c and d).

The report of Water Resources Angecy proposed that crop water requirement minus effective rainfall throughout the whole paddy growth season should range between 1136 - 1317 mm in Changhua and Yunlin area (Kan 2002). If considering conveyance loss, the proposed irrigation consumption will be approximately 1550 - 1800 mm. Following the standard, the irrigation water requirement estimation (Fig. 8) is reasonable when using the water balance model. Excluding 2002, 2005, and 2006, the differences in Changhua between the observations and estimations in the first and second paddy growth seasons are 11.4 and 14.8%, respectively. The differences in Yunlin are 13.9 and 17.0%, respectively.

Currently, the planned farming areas in Changhua in the first and second paddy growth seasons are 370.3 and 390.8 km^2, respectively. The areas in Yunlin are 106.7 and 369.9 km^2, respectively. By multiplying the estimated values from 2001 - 2010, the annual irrigation volume requirement is nearly 1.9 billion m^3, which is close to the annual irrigation supply from the Jiji division weir at 1.8 billion m^3.

3.3 Tank Model Validation

Wushe, Tanchung, Chenyulan, and Chingshui are the four sub-basins selected for constructing the tank model for the Zhoshui River basin (Fig. 1). The river flow gauges at these four sub-basins are unaffected by water-related infrastructures such as reservoirs. These sub-basins cover about 60% of the basin area. In the rest of the area, the area ratio is applied to estimate river flow. For example, the Chingshui River flow below the Tungtou weir (154 km^2) is equal to 0.59 times the Tungtou weir flow (259 km^2).

We used 8-yr data for parameter calibration and the remaining 2 years (2009 - 2010) for verification. Table 3 shows the tank model calibrated parameters. The annual differences in volume in the four main sub-basins are verified

between 3.7 - 13.1%. In addition, the bias throughout the wet season (May - October) is higher than in the dry season (November - April), except in the Tanchung sub-basin (Table 4). Figure 9 shows the daily discharge validation in the sub-basins and demonstrates that the tank model is able to simulate the river flow characteristics in these sub-basins. In addition, when applying the tank model we assumed that the watershed characteristics will remain unchanged in the future—in other words, that the parameters identified for the current climate will remain valid.

4. RESULTS AND DISSCUION

4.1 Projection of Meteorological Data

Figure 10 illustrates the temporal precipitation and temperature distributions. Note that the meteorological data in the Zhoshui River basin are a weighted average of the sub-basins.

According to precipitation projections, the annual precipitation in the Zhoshui basin in the future (2046 - 2065) will range from 2104.0 - 2489.9 mm, with an average of 2287.5 mm. Based on the current annual precipitation (2469.7 mm for 2001 - 2010), most GCMs project a decrease in the future (-14.8 - 0.8%). On average, the precipitation projections are 7.4% lower than at present. However, the temporal precipitation distribution in the Zhoshui basin indicates that more fluctuations would occur in each month, especially in July and August (see top left graph of Fig. 10).

The precipitation projections for the upstream and downstream areas are similar. However, the monthly precipitation distribution in the future has obvious fluctuations. As the top center and top right graphs of Fig. 10 indicate, the temporal precipitation distribution will be more uneven in both areas in the future. The difference between the average annual precipitation in the present and future is insignificant. The present annual precipitation levels in Changhua and Yunlin are 1435.9 and 1878.7 mm, respectively. For Changhua, the variations in projections of annual precipitation are between -241.9 and 260.1 mm (-16.8 - 18.1%), with an average of 33.4 mm (2.3%). For Yunlin, the variations in projections of annual precipitation are between -270.1 and 578.8 mm (-14.4 - 30.8%), with an average of 49.6 mm (2.6%).

Temperature projections for the Zhoshui basin show

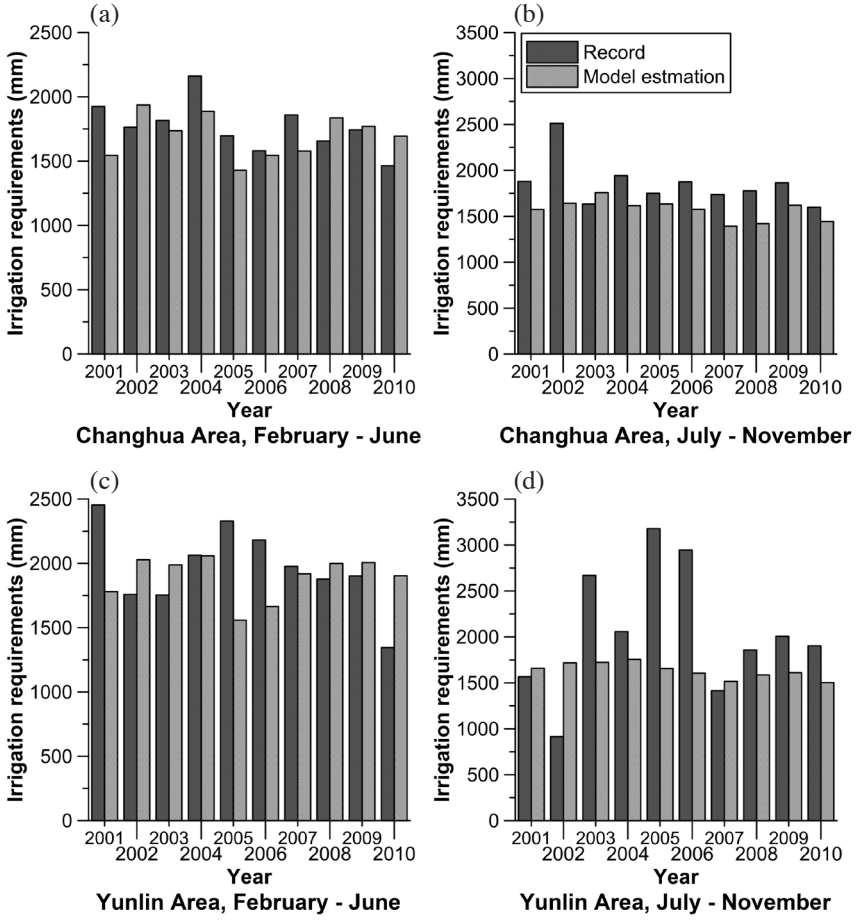

Fig. 8. Comparison of paddy water requirements between recorded consumption and model estimation in 2001 - 2010: (a) Changhua area in February - June; (b) Changhua area in July - November; (c) Yunlin area in February - June; (d) Yunlin area in July - November.

Table 3. Result of calibration for four main sub-basins of the Zhoshui River.

Sub-Basins	Orifice coefficient (10^{-3} day^{-1})				Orifice height (mm)	
	a_0	a_1	a_2	b_1	h_1	h_2
Wushe	9.8	17.7	121.5	18.0	13.9	151.1
Tanchung	38.1	13.3	63.9	15.3	0.0	112.7
Chenyulan	40.3	57.4	156.0	12.4	18.9	118.6
Chingshui	10.4	177.7	394.3	28.0	61.5	149.5

Table 4. Tank model validation in volume error for four main sub-basins of the Zhoshui River in 2009 - 2010 (unit in %).

	Wushe	Tanchung	Chenyulan	Chingshui
Whole year	+13.1	+3.7	+10.8	+11.9
Wet season	+14.5	+2.1	+11.4	+13.1
Dry season	+8.8	+9.5	+8.5	-7.9

Note: "+" means overestimation; "-" means underestimation.

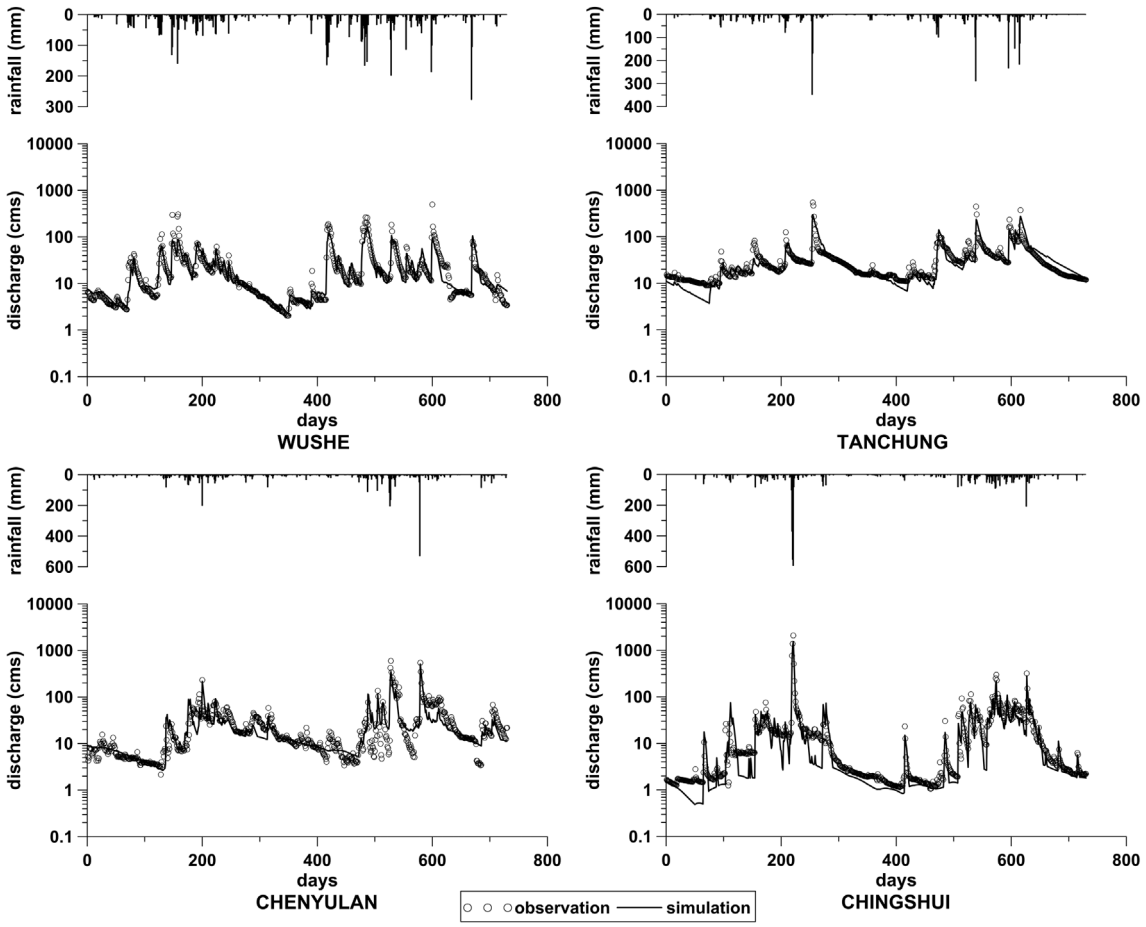

Fig. 9. Comparison of daily discharge between observation and tank model projection for four main sub-basins of the Zhoshui River in 2009 - 2010.

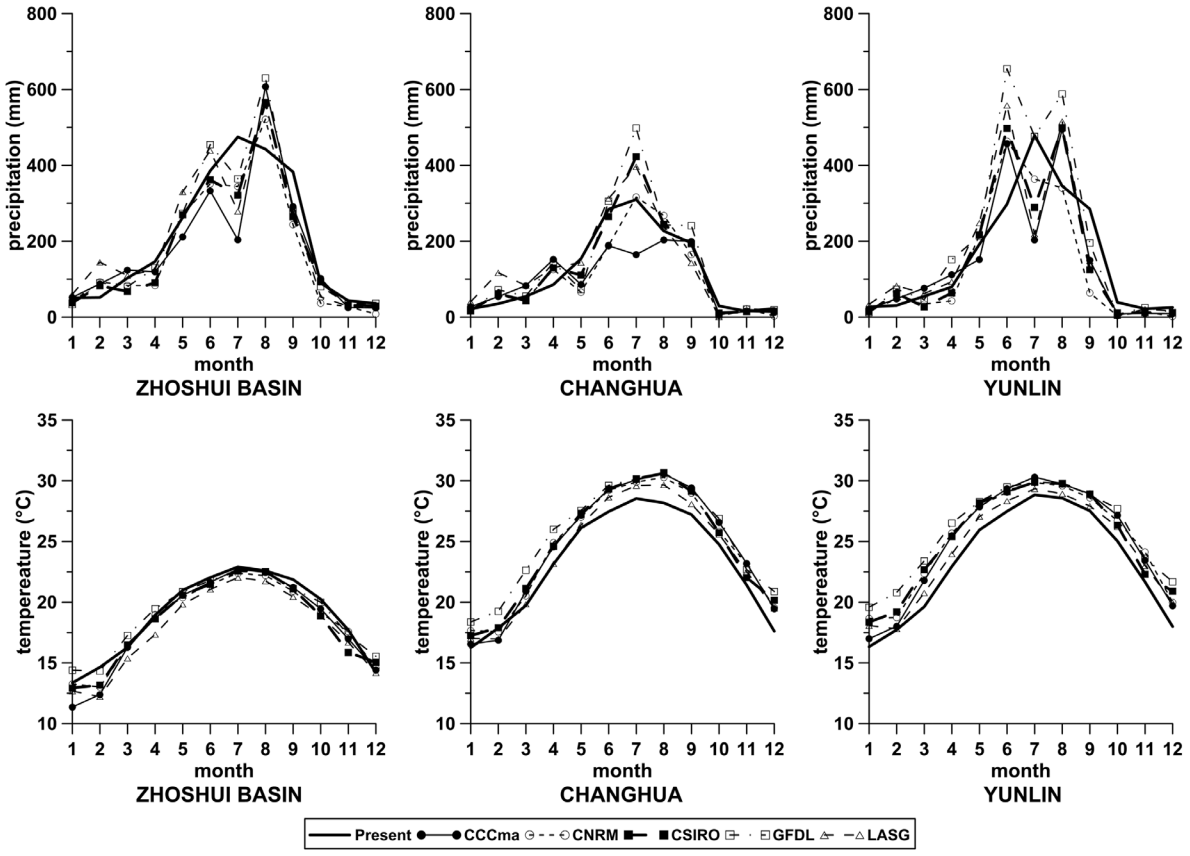

Fig. 10. Comparison of precipitation and temperature between the present (2001 - 2010) and future (2046 - 2065).

that the difference in the annual mean between the present and future is insignificant. The weighted annual temperature average in the Zhoshui basin is currently 18.8°C. The variations in projections are between -1.1 and 0.1°C (-5.9 - 0.6%), and the average decrease in the future is 0.5°C (2.8%). By contrast, the variations in temperature projections for Changhua and Yunlin are significant. For Changhua, the increment in annual mean temperature projections range from 0.7 - 2.1°C (3.1 - 9.2%), with an average of 1.4°C (6.0%). For Yunlin, the increment in annual temperature projections range from 1.0 - 2.5°C (4.2 - 10.7%), with an average of 1.7°C (7.4%). Both areas exhibit increasing tendencies.

4.2 Impact of Climate Change on Irrigation Water Requirements

Table 5 shows that, compared with the present irrigation requirement (2001 - 2010), the projected irrigation water requirement for 2046 - 2065 increases slightly, within the range of 19.4 - 155.6 mm (1.2 - 9.5%). GCMs projections indicate that the monthly mean temperature in the future will increase 0.5 - 3.0°C on average, as shown in Fig. 10. Rising temperature will certainly cause crop water requirements (ET_c) to increase during 2046 - 2065. The increments of ET_c are within 85.0 - 132.4 mm (16.1 - 22.0%) throughout each paddy growth season in the Changhua and Yunlin areas.

However, rising temperatures associated with GDDs will reduce the growth duration. Compared to the present growth duration, the future growth duration of paddy crops will decrease by 5.2 - 10.7 days in both areas. Hence, there is a marked increment in ET_c, but the irrigation requirement increment will be smaller than 10% in the future.

4.3 Impact of Climate Change on River Flow

In 2046 - 2065, the annual precipitation in these sub-basins will decrease, except in Wushe. On average, the projected annual precipitations in the Tanchung, Chenyulan, and Chingshui sub-basins decrease by 404.4, 439.1, and 22.4 mm (20.9, 17.9, and 0.7%), respectively. Wushe is projected to increase by 754.2 mm (24.9%) in the future. Consequently, the variations in projected annual discharge in the sub-basins are approximately -272 - 3 million m^3 (-33.3 - 0.5%). Figure 11 shows a comparison of temporal distributions of river flow between the present and future. Overall, an obvious decrease will occur in the discharge of the Zhoshui River from July to December.

Table 5. Annual irrigation water requirement during the present (2001 - 2010) and the future (2046 - 2065).

Irrigation water requirement (mm)	Cropping seasons	Present	Future					
			CCCma	CNRM	CSIRO	GFDL	LASG	Average
Changhua Area	February - June	1696	1749	1832	1744	1663	1660	1730
	July - November	1568	1595	1598	1583	1454	1707	1587
Yunlin Area	February - June	1890	1994	2064	2017	1857	1863	1959
	July - November	1633	1750	1887	1781	1656	1869	1789

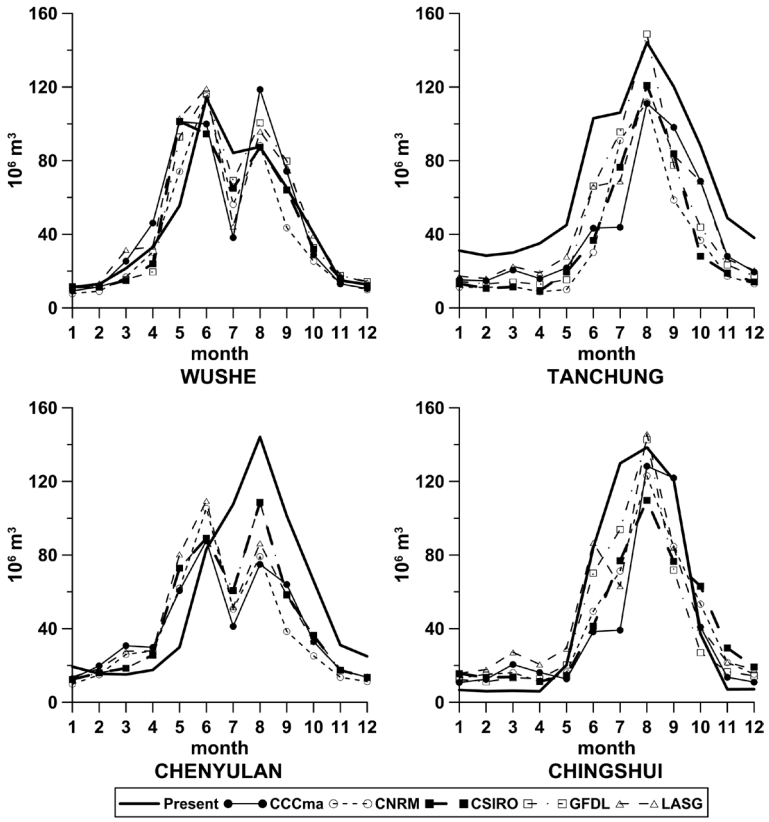

Fig. 11. Comparison of river flow of sub-basins between the present (2001 - 2010) and future (2046 - 2065).

4.4 Impact of Climate Change on the Water Supply and Benefits of Hushan Reservoir

In the following section, we assume that the industrial and domestic demands will remain the same in the present (2001 - 2010) and future (2046 - 2065). The daily industrial and domestic demands are 3.5×10^5 and 2.0×10^5 m^3, respectively.

Although the Hushan Reservoir operational regulations are not yet stipulated, we assume that the Hushan Reservoir will be responsible for supplying all domestic demand because the Zhoshui River sediment concentration is always high. In addition, this reservoir must draw water from Chingshui Creek without affecting irrigation demand downstream.

Table 6 shows the water supply situation before and after building the Hushan Reservoir. The Hushan Reservoir clearly aids domestic supply. Future water shortages for irrigation and industry are exacerbated because of river flow reductions throughout the Zhoshui River basin (the decrement is 20.4% according to the weighted average; see section 4.3). On average, the annual irrigation and industry deficit increases by 159.2 and 4.5 million m^3, maximum consecutive water-shortage days for irrigation and industry increase by 2 - 4 times, and the shortage index for industry is raised to 3.7 from 2.5. Moreover, the satisfaction and reliability temporal distributions indicate that water shortages from September to February in subsequent years will be more severe than those at present (Figs. 12 and 13).

Domestic demand could be fully satisfied when

Table 6. Results of water supply simulation.

		Without Hushan in 2001 - 2010	With Hushan in 2046 - 2065					
			CCCma	CNRM	CSIRO	GFDL	LASG	Average
Annual deficit (10^6 m^3)	Irr.	456.4	548.0	803.1	651.0	478.1	597.4	615.6
	Ind.	18.3	17.9	31.0	25.9	21.6	17.4	22.8
	Dom.	11.2	0.0	0.0	0.0	0.0	0.0	0.0
Maximum consecutive water-shortage days	Irr.	57.0	117.0	166.0	116.0	87.0	105.0	118.2
	Ind.	20.0	116.0	114.0	54.0	80.0	54.0	83.6
	Dom.	63.0	0.0	0.0	0.0	0.0	0.0	0.0
Shortage index	Ind.	2.5	2.0	6.4	4.3	3.1	2.5	3.7
	Dom.	4.1	0.0	0.0	0.0	0.0	0.0	0.0

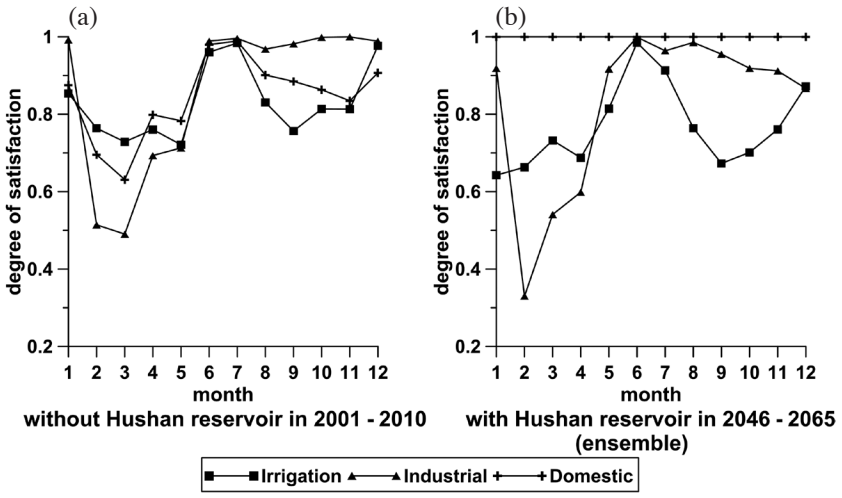

Fig. 12. Monthly Degree of Satisfaction: (a) without Hushan reservoir in the Present; (b) with Hushan reservoir in the future.

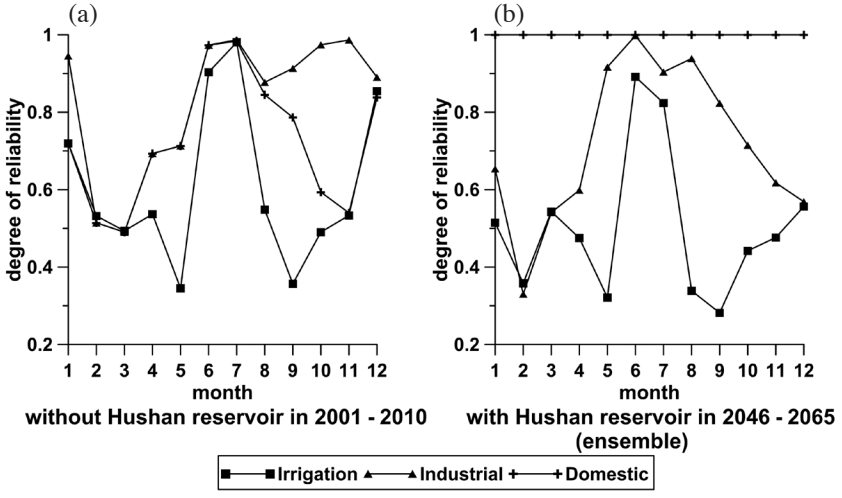

Fig. 13. Monthly Degree of Reliability: (a) without Hushan Reservoir in the Present; (b) withe Hushan reservoir in the future.

the Hushan Reservoir begins operation (Table 6; Figs. 12 and 13). This result demonstrates that the new reservoir achieves its original objective to stabilize the domestic water supply. However, we found that Hushan Reservoir would release only 25.4 million m^3 per year in the future. This annual release is approximately 50% of the reservoir's capacity (52 million m^3). To enhance the Hushan Reservoir utilization efficiency, alternatives should be evaluated that assist other water users.

4.5 Adaptations for Industrial and Irrigation Demands

Because different GCMs produce different patterns of change in temperature and precipitation, multi-ensemble runs instead of single GCMs were used to reduce uncertainties. Therefore, the results show an average of all GCM simulations.

Compared with domestic demand, future irrigation and industrial demand will encounter higher pressures than at present. The first adaptation indicates that the Hushan Reservoir could significantly support industrial demand in the future without affecting domestic use. Comparing the industrial demand indices with the future average in Table 6 and case (a) in Table 7, in which the annual shortage drops from 22.8 - 0.3 million m^3, indicates that maximum consecutive water-shortage days would decrease to 7.2 from 83.6 days, and the shortage index would decline to 0.02. The temporal satisfaction degree distributions [part (b) in Fig. 12 vs. part (a) in Fig. 14] and reliability degree [part (b) in Fig. 13 vs. part (a) in Fig. 15] indicate that these industrial supply indices will be higher than 90% in the future. Consequently, the Hushan Reservoir utilization efficiency will increase after supporting industrial demand. The future annual Hushan Reservoir release increases to 47.7 million m^3, compared to 25.4 million m^3 per year at present.

Currently, the conveyance losses due to irrigation in the Changhua and Yunlin areas are 40.7 and 36.0%, respectively. These values are higher than the average loss in Taiwan. The second adaptation further reduces the irrigation conveyance loss in both areas to an average of 30%. Case (b) in Table 7, and Figs. 14 and 15 show the water supply simulations after reducing conveyance loss. By comparing cases (b) and (a), we find that the annual irrigation deficit decreases by 83.0 million m^3 (13.5%). Additionally, the number of maximum consecutive water-shortage days decrease to 95.8 days from 118.2 days, and the satisfaction and reliability degree from September to December also improves. However, Alternative 2 is unable to return to the deficit level prior to the Hushan operation. The annual shortage at that time was approximately 456.4 million m^3 per year [case (a), Table 6].

Crop rotation or fallow fields are options for saving water during shortages. According to the simulation results shown in Table 6 (in the case of without Hushan in 2001 - 2010) and Table 7 case (b), an extra 76.2 million m^3 deficit occurs after improving irrigation conveyance loss. We considered applying area reduction as a possible alternative to offset future water deficits. Using trial and error, we found that reducing farming areas by 10% in the second paddy growth season would allow the annual irrigation deficit to return to the present level. According to case (c) in Table 7, the annual irrigation deficit would drop to 457.0 million m^3 if the adaptations were applied. However, indices such as irrigation satisfaction and reliability [case (c), Figs. 14 and 15] would not return to the present level [case (a) in Figs. 12 and 13]. These indices are affected mainly by climate change.

5. CONCLUSIONS

The impact of climate change on water resources is of high concern. However, the limitations imposed by hydrological spatial and temporal variation conditions and the

Table 7. Results of water supply simulation of adaptations in 2046 - 2065.

Indices of assessment	Kinds of demand	Adaptations		
		(a)	(b)	(c)
Annual deficit (10^6 m^3)	Irrigation	615.6	532.6	457.0
	Industrial	0.3	0.2	0.2
	Domestic	0.0	0.0	0.0
Maximum consecutive water-shortage days	Irrigation	118.2	95.8	91.8
	Industrial	7.2	5.6	6.6
	Domestic	0.0	0.0	0.0
Shortage index	Industrial	0.02	0.01	0.01
	Domestic	0.0	0.0	0.0

Note: (a) Hushan supports industrial demand; (b) Hushan supports industrial demand and conveyance loss of irrigation reduces to 30%; (c) further reduces 10% of irrigation area in second cropping season.

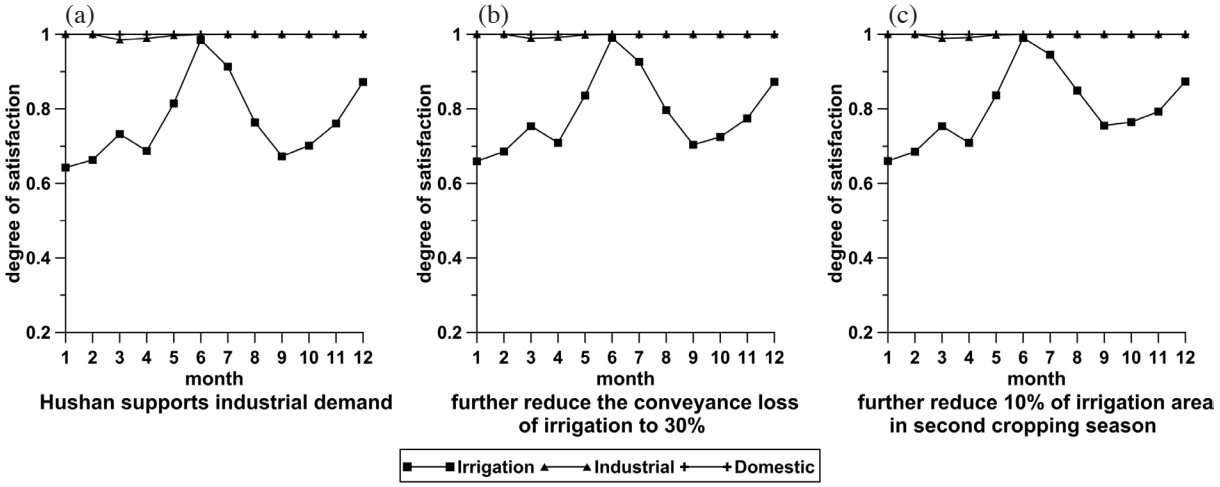

Fig. 14. Degree of satisfaction for adaptations in 2046 - 2065: (a) if Hushan supports industrial demand; (b) if further reduce the conveyance loss of irrigation to 30%; (c) if further reduce 10% of irrigation area in second cropping season.

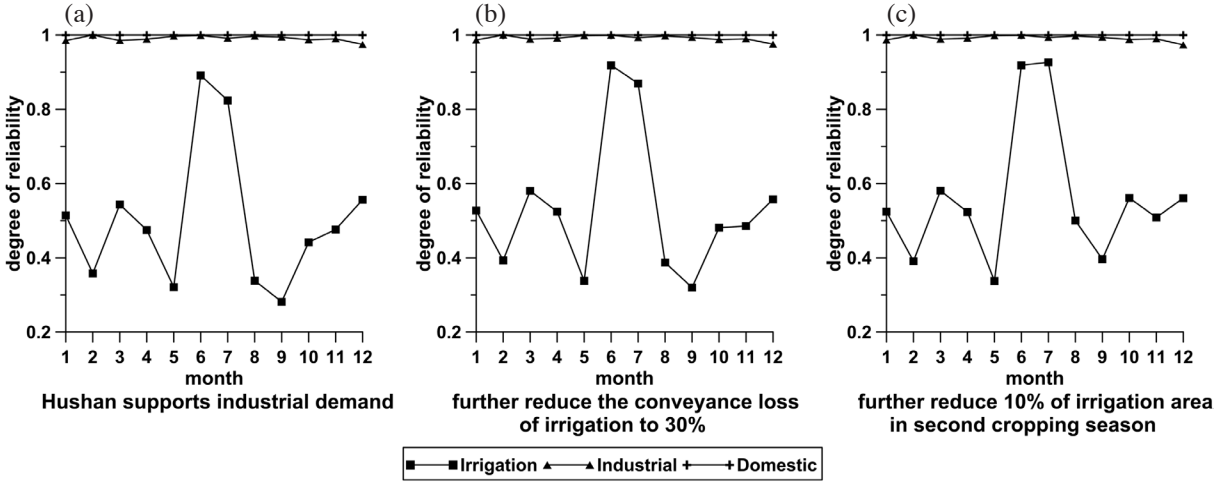

Fig. 15. Degree of reliability for adaptations in 2046 - 2065: (a) if Hushan supports industrial demand; (b) if further reduce the conveyance loss of irrigation to 30%; (c) if further reduce 10% of irrigation area in second cropping season.

complexity of human intervention effects in the environment hinder estimation (Rees et al. 1997). This study investigated the impact of climate change on water resources within the period 2046 - 2065. The Zhoshui River basin in Central Taiwan was selected for analysis.

This paper demonstrates an integrated procedure for assessing water resources system response to climate change on the basin scale, and provides a reference for people concerned with local scale planning practices related to the impact of climate change. Bias correction was attained using a quadrant transformation method. A two-layer tank model was used for rainfall-runoff estimation. A water balance model for paddy fields was proposed for simulating irrigation water requirements. The applicability of these models was demonstrated in this study.

Comparison of the projections from 2001 - 2010 and 2046 - 2065 suggests that future irrigation water requirements will increase 10% less in each cropping season in the Changhua and Yunlin areas. However, future river flow in the Zhoshui basin will decrease by approximately 20%. Consequently, water shortage is inevitable, particularly from September to February, owing to irrigation. Thus, climate change will have a considerable impact on water supply, particularly in the agricultural sector. The annual deficit associated with irrigation and industrial demand may increase by 30% compared to the present levels, and the maximum number of consecutive water-shortage days will nearly double.

Adaptations were introduced to alleviate the impacts of climate change on water resources. Domestic demand will be fully met after the Hushan Reservoir comes on-line in mid-2016. Furthermore, the industrial water shortage can be

substantially reduced without affecting domestic demand if the Hushan Reservoir can support it.

Alternatively, reducing irrigation conveyance losses and farming areas are effective ways to mitigate water shortages for irrigation in the future. We recommend reducing conveyance loss by 30% and cutting farming areas by 10% in the second paddy growth season to mitigate future annual irrigation deficits and retain deficits at the present level.

Acknowledgements The authors thank the National Taiwan University Global Change Center for providing relevant meteorological projections. This study was sponsored by the Ministry of Science and Technology, Taiwan in 2012 - 2014 (NSC 101-2625-M-019-003, MOST 102-2625-M-019-001, and MOST 103-2625-M-019-001).

REFERENCES

Allen, R. G., L. S. Pereira, D. Raes, and M. Smith, 2006: Crop Evapotranspiration - Guidelines for Computing Crop Water Requirements - FAO Irrigation and Drainage Paper 56, FAO - Food and Agriculture Organization of the United Nations, Rome.

Chen, R. S., L. C. Pi, and C. C. Hsieh, 2005: Application of parameter optimization method for calibrating tank model. *J. Am. Water Resour. Assoc.*, **41**, 389-402, doi: 10.1111/j.1752-1688.2005.tb03743.x. [Link]

Eskridge, K. M. and E. J. Stevens, 1987: Growth curve analysis of temperature-dependent phenology models. *Agron. J.*, **79**, 291-297, doi: 10.2134/agronj1987.00021962007900020023x. [Link]

Gilmore, E. C. and J. S. Rogers, 1958: Heat units as a method of measuring maturity in corn. *Agron. J.*, **50**, 611-615, doi: 10.2134/agronj1958.00021962005000100014x. [Link]

Hardke, J., C. E. Wilson, Jr., and R. Norman, 2013: DD50 computerized rice management program. In: Hardke, J. T. (Ed.), Arkansas Rice Projection Handbook - MP192, University of Arkansas Cooperative Extension Service Print Media Center, Little Rock, Arkansas, U.S.A., 45-51.

Hodges, T., 1991: Temperature and water stress effects on phenology. In: Hodges, T. (Ed.), Predicting Crop Phenology, CRC Press, Florida, U.S.A., 8-9.

Hsu, H. H., C. Chou, Y. Wu, M. M. Lu, C. T. Chen, and Y. M. Chen, 2011: Climate Change in Taiwan: Scientific Report 2011 (Summary), National Science Council, Taipei, Taiwan.

Hualien District Agricultural Research and Extension Station, 2006: Annual Report, Hualien District Agricultural Research and Extension Station, Council of Agriculture, Executive Yuan, Taiwan. (in Chinese)

Hualien District Agricultural Research and Extension Station, 2007: Annual Report, Hualien District Agricultural Research and Extension Station, Council of Agriculture, Executive Yuan, Taiwan. (in Chinese)

Huang, W. C., Y. Chiang, R. Y. Wu, J. L. Lee, and S. H. Lin, 2012: The Impact of Climate Change on Rainfall Frequency in Taiwan. *Terr. Atmos. Ocean. Sci.*, **23**, 553-564, doi: 10.3319/TAO.2012.05.03.04(WMH). [Link]

Huang, W. C., Y. H. Wu, and J. L. Lee, 2014a: Impact of climate change on rainfall in Taiwan during 2046-2065. *J. Taiwan Agric. Eng.*, **60**, 66-80. (in Chinese)

Huang, W. C., T. Y. Chu, and J. L. Lee, 2014b: Impact on water supply under climate change for Shihmen Reservoir. The 13th Conference of International Society of Paddy and Water Environment Engineering, Kaohsiung, Taiwan.

Hung, W. C., C. Hwang, J. C. Liou, Y. S. Lin, and H. L. Yang, 2012: Modeling aquifer-system compaction and predicting land subsidence in central Taiwan. *Eng. Geol.*, **147-148**, 78-90, doi: 10.1016/j.enggeo.2012.07.018. [Link]

IPCC, 2007: Climate Change 2007: Synthesis Report. In: Core Writing Team, R. K. Pachauri, and A. Reisinger (Eds.), Contribution of Working Groups I, II and III to the Fourth Assessment Report of the Intergovernmental Panel on Climate Change, IPCC, Geneva, Switzerland.

Kalnay, E., M. Kanamitsu, R. Kistler, W. Collins, D. Deaven, L. Gandin, M. Iredell, S. Saha, G. White, J. Woollen, Y. Zhu, M. Chelliah, W. Ebisuzaki, W. Higgins, J. Janowiak, K. C. Mo, C. Ropelewski, J. Wang, A. Leetmaa, R. Reynolds, R. Jenne, and D. Joseph, 1996: The NCEP/NCAR 40-year reanalysis project. *Bull. Amer. Meteorol. Soc.*, **77**, 437-471, doi: 10.1175/1520-0477(1996)077<0437:TNYRP>2.0.CO;2. [Link]

Kan, C. E., 2002: Study on the Effective Use Strategies of Agricultural Conserved Water, Water Resources Agency, Ministry of Economic Affairs, Taiwan.

Lee, J. L. and W. C. Huang, 2014: Impact of climate change on the irrigation water requirement in northern Taiwan. *Water*, **6**, 3339-3361, doi: 10.3390/w6113339. [Link]

Lee, K. T., 1993: Tank Model and Rainfall-Runoff Simulation. *J. Taiwan Agric. Eng.*, **39**, 20-28. (in Chinese)

Lin, S. H., Y. C. Chen, W. S. Lin, and C. M. Liu, 2009: Climate change projection for Taiwan based on statistical downscaling on daily temperature and precipitation. The 15th International Joint Seminar on the Regional Deposition Processes in the Atmosphere and Climate Change, Taipei, Taiwan.

Lin, S. H., C. M. Liu, W. C. Huang, S. S. Lin, T. H. Yen, H. R. Wang, J. T. Kuo, and Y. C. Lee, 2010: Developing a yearly warning index to assess the climatic impact on the water resources of Taiwan, a complex-terrain island. *J. Hydrol.*, **390**, 13-22, doi: 10.1016/j.jhydrol.2010.06.024. [Link]

Miller, P., W. Lanier, and S. Brandt, 2001: Using Growing Degree Days to Predict Plant Stages, Montana State University Extension Service, Montana, U.S.A.

Nakicenovic, N. and R. Swart, 2000: Special Report on Emissions Scenarios, Cambridge Univ. Press, U.K.

Powell, M. J. D., 1964: An efficient method for finding the minimum of a function of several variables without calculating derivatives. *Comput. J.*, **7**, 155-162, doi: 10.1093/comjnl/7.2.155. [Link]

Rees, H. G., K. M. Croker, N. S. Reynard, and A. Gustard, 1997: Estimation of renewable water resources in the European Union. FRIEND'97—Regional Hydrology: Concepts and Models for Sustainable Water Resource Management, Proceedings of the Postojna, Slovenia, Conference, IAHS Publ., no. 246, 31-38.

Russelle, M. P., W. W. Wilhelm, R. A. Olson, and J. F. Power, 1984: Growth analysis based on degree days. *Crop Sci.*, **24**, 28-32, doi: 10.2135/cropsci1984.0011183X002400010007x. [Link]

Searcy, J. K., 1959: Flow-duration curves. Manual of Hydrology: Part 2, Low-Flow Techniques, United States Department of the Interior, Washington, U.S.A.

Shaw, S. B. and S. J. Riha, 2011: Assessing temperature-based *PET* equations under a changing climate in temperate, deciduous forests. *Hydrol. Process.*, **25**, 1466-1478, doi: 10.1002/hyp.7913. [Link]

Shih, C. C. C., Y. P. Hsu, Y. S. Cao, and C. E. Kan, 1996: Principles of Irrigation and Drainage, Central Book Publishing, Taipei, Taiwan, 227. (in Chinese)

Sugawara, M., 1961: On the analysis of runoff structure about several Japanese rivers. *Jpn. J. Geophys.*, **2**, 1-76.

Tanakamaru, H., 1995: Parameter estimation for the tank model using global optimization. *Trans. JSIDRE*, **178**, 103-112, doi: 10.11408/jsidre1965.1995.503. [Link]

The University of Adelaide, Flinders University, and The University of Waikato, 2009: Identifying hot spots of climate change impact. Climate Change and Migration in Asia and the Pacific, Asian Development Bank, Mandaluyong City, Philippines, 15-18.

Tung, H. and J. C. Hu, 2012: Assessments of Serious Anthropogenic land subsidence in Yunlin County of central Taiwan from 1996 to 1999 by Persistent Scatterers InSAR. *Tectonophysics*, **578**, 126-135, doi: 10.1016/j.tecto.2012.08.009. [Link]

Yokoo, Y. and S. Kazama, 2012: Numerical investigations on the relationships between watershed characteristics and water balance model parameters: Searching for universal relationships among regional relationships. *Hydrol. Process.*, **26**, 843-854, doi: 10.1002/hyp.8299. [Link]